Denoising of Mammographic Images from Quantum Noise in Wavelet Domain

Smriti Bhatnagar, Richa Gupta

***Abstract*: *Telemedicine is the new trends in Health care services. Advances in Electronics, Imaging Techniques and Communication Engineering help a lot in early diagnosis and fast recovery of some fatal diseases. As an example case of breast cancer is considered here. Digital Mammographic images are used for diagnosis of Breast cancer. But they are contaminated by quantum noise during acquisition due to the nature of low energy photons used for Mammographic imaging modality. To remove the Quantum Noise in mammographic images, use of Discrete Wavelet Transforms (DWT) is gaining momentum due to unique properties of sparcity and multiresolution and easy implementation of DWTs with different Digital Filters. Thresholding techniques such as VisuShrink, BayesShrink, NeighShrink and Modified Neighbourhood are used in this paper and three different wavelets as Haar, Db4 and Sym4 has been used. The Performance Metrics such as Peak Signal to Noise Ratio(PSNR), Mean square Error(MSE), Structural Similarity Index (SSIM) and Edge Preserving Index (EPI) are used to evaluate the performance of Denoising algorithms*.**

***Index Terms:* *Tele mammograph; Discrete Wavelet Transform(DWT); Denoising; Thresholding*.**

I. INTRODUCTION

Telemedicine and Tele health care systems are the demand and need of the day. These systems are properly coordinating and facilitating the advances in computer and informatics to the health care for the accurate and speedy diagnosis and recovery of patients. Due to advances in the area like Internet of Things, it is possible for a patient living in the remote and undeveloped area, to get most expert advice across the globe and that too with a small cost and time. Tele mammography is one of such health care service for early diagnosis of breast cancer, which is a major cause of deaths [1] in women aged between forty to seventy years. Prevention seems impossible for this disease, as the cause is still unknown. Early detection is the only way to reduce risk and mortality. The improvement in the imaging technology increases the chances of survival. Improvement not only in technology but also in reducing the cost and availability of clinical procedure is required for the betterment of humanity. The mammography is one such technique, using X-Ray for forming the image of the breast. Screening mammography and diagnosis mammography are two different methods, one is for the routine check up and other is for positive cases of breast cancer. Now a day's Digital Mammography is used instead of Film Mammography to facilitate the digital transmission and storage of these images[2]-[3], which is essential for telemedicine and healthcare systems. Digital Mammography uses the lesser dose of radiation as compared to Film mammography. In the process of acquiring, transmitting and archiving, noise is added to these images and can result in miss leading information. The type of the noise in mammographic images is of quantum [4] in nature because of low count X-Ray photons, and best represented by Poisson's Distribution shown in Fig . 1

Revised Manuscript Received on 30 May 2019.
***** Correspondence Author
Smriti Bhatnagar*, ECE Department , Japee Institute of Information Technology, Noida,
Richa Gupta , ECE Department , Japee Institute of Information Technology, Noida,

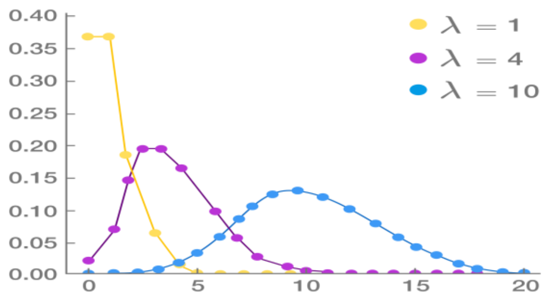

Fig . 1: Poisson's Distribution

$$P(x,\lambda) = \frac{e^{-\lambda}\lambda^{x}}{x!} \qquad x= 1,2,3...... \qquad (1)$$

$\mu = \lambda$ Mean ,

$\sigma = \sqrt{\lambda}$ Stand. Deviation and

$\sigma^2 = \lambda$ Variance

as λ increases in Eq. (1), the distribution changes to Gaussian.

Poisson's noise affects with very small variations, all the pixels of an images. It's presence is difficult to recognise by eyes in mammographic images but it adversely affects the distinction between benign, micro calcification and malignant portion of the images. It is very difficult to differentiate between micro calcification and high frequency noise due to their small size. Denoising as a pre-processing becomes mandatory here for reliable diagnosis of disease. Wavelet Transform is one of the powerful tools used to give the way to access and detect information appearing at different scales, level and selectivity. Translation variance is the basic drawback of wavelet transform techniques but can be overcome by using un decimated wavelet transform as at the cost of increased redundancy [5-9].

Organisation of the paper as follows section 2, gives the idea of scheme for denosing, section 3 gives the mathematical concepts of the wavelet transforms. Section 4 provides the idea about shrinkage function and threshold selection for Denoising the quantum noise of Mammographic images. Section 5 and Section 6 give the results, discussions and conclusions.

II. DENOISING SCHEME

A Common scheme for Denoising using Discrete Wavelet Transform has following steps

- Wavelet Decomposition of the Corrupted (Poisson's noise) Mammographic Image
- Threshold selection and modification of wavelet coefficients with selected scheme [10]
- Image Reconstruction with these modified wavelet coefficients .

Here the paper includes the wavelet transform of different families

- Haar,
- Daubechies ,
- Symlets

Denoising with four different wavelet shrinkage functions

- Visu Shrink ,
- Bayes Shrink,
- Neighbourhood Shrink,
- Modified Neighbourhood Shrink.

Different schemes have been compared on the basis of performance indices PSNR, MSE, SSIM and EPI. Time is also measured and compared for different methods.

III. MATHEMATICAL CONCEPT

After selecting a particular wavelet function, it can be implemented with the help of two parameters : translation and scaling. The translation means the shifting of the central position of the mother wavelet along the time axis and the scaling means either the stretching or compressing the mother wavelet in time domain. When the process of translation and scaling are done in discrete steps then it's called Discrete Wavelet Transform. Wavelet function is mathematically represented as in (2).

$$\psi_{\tau,s}(t) = \frac{1}{\sqrt{s}}\psi\left(\frac{t-\tau}{s}\right) \qquad (2)$$

τ = translation or location shift and s = scaling factor.
Wavelet transform of a function f(t) is given in (3)

$$W(\tau,s) = \int f(t)\,\frac{1}{\sqrt{s}}\psi\left(\frac{t-\tau}{s}\right)dt \qquad (3)$$

Two sets of functions namely wavelet functions (mother wavelet) ψ(t) and scaling functions φ(t) are used to decompose the signal and these functions are complementary to each other [5]. Mother wavelet follows the following properties

$$\int_{-\infty}^{\infty}\psi(t)dt = 0$$

$$\int_{-\infty}^{\infty}|\psi(t)|^{2}dt = 1$$

Function f(t) can be represented in terms of mother wavelet for different resolution by

$$W(j,k) = \int f(t)2^{j/2}\psi(2^{j}t - k)\,dt \qquad (4)$$

$$\psi_{j,k}(t) = 2^{j/2}\psi(2^{j}t - k) \qquad (5)$$

$$\psi_{0,0}(t) = \psi(t) \qquad (6)$$

Where s and τ are defined as $s = 2^{j/2}$ and $\tau = k2^{j/2}$, j and k are integers for DWT.

By using two variables representation, a sufficient amount of redundancy is used to retain the local properties of original signal. A fast computation of DWT is possible by implementing the scaling function equation Equations and wavelet function equations in different subspaces with the help of convolution and filter bank concept of signal processing. This is the main reason of use of wavelets in signal processing [8,9,11].

Sets of coefficients h(k) and g(k) act as low pass and high pass filter coefficients respectively.

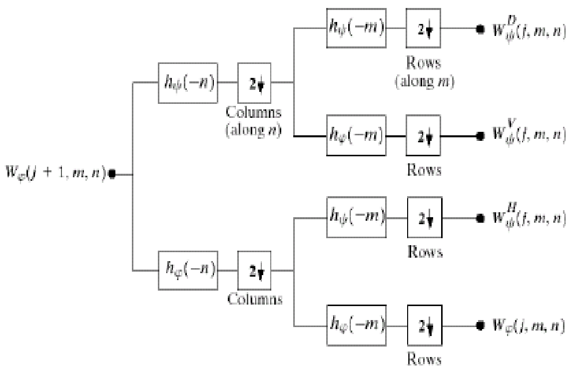

Fig. 2(a) : Decomposition of image

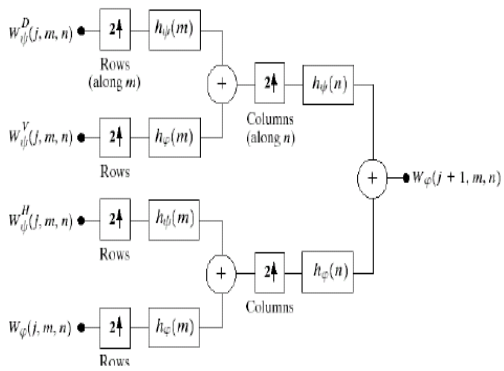

Fig. 2(b): Reconstruction of image

IV. DIFFERENT SHRINKAGE FUNCTION AND EVALUATION PARAMETERS

Different shrinkage functions are described [6-7] as

4.1. Visual Shrink

Threshold T can be calculated using the formulae,

$$T = \sigma\sqrt{2\log n^2} \tag{7}$$

Where σ is the variance , which is signal dependent for the Poisson's Distribution.

4.2. Bayesian or Normal Shrink

calculates the threshold value (T_N), which is adaptive to different sub band characteristics

$$T_N = \frac{\beta\sigma^2}{\sigma_y} \tag{8}$$

where the scale parameter β is computed once for each scale using the following relation : $\beta = \sqrt{\frac{L_k}{j}}$. L_k is the length of the sub band at k^{th} scale, σ^2 is the noise variance, which is estimated from the sub band HH_1, using the

$$\hat{\sigma}_y{}^2 = \left[\frac{medain(|Y_{ij}|)}{0.625}\right]^2, |Y_{ij}| \in subband\,HH \tag{9}$$

Where $\hat{\sigma}_y{}^2$ is the standard deviation of the sub band under consideration.

4.3. Bayesian or Normal Shrink

Let d(i,j) denotes the wavelet coefficients of interest then d(i,j) = d(i,j) * B(i,j), where

$$B(i,j) = (1 - \frac{\tau^2}{s^2(i,j)})\ and\ s^2 = \sum d^2(i,j) \tag{10}$$

4.4. Modified Neighbour Shrink

This is same as Neighbour Shrink except

$$B(i,j) = (1 - 0.75 * \frac{\tau^2}{s^2(i,j)})\ and\ s^2 = \sum d^2(i,j) \tag{11}$$

4.5. Evaluation Parameters

1) The objective quality of reconstructed image is measured by:

$$PSNR = 10\log_{10}\frac{255^2}{MSE} \tag{12}$$

where MSE is mean square error between original(x) and denoised image(x^)

$$MSE = \frac{1}{MXN}\sum_{i=1}^{M}\sum_{j=1}^{N}\left(x(i,j) - \hat{x}(i,j)\right)^2 \tag{13}$$

$$\mathrm{SSIM(x,y)} = \frac{(2\mu_x\mu_y + C_1)(2\sigma_{xy} + C_2)}{(\mu^2{}_x + \mu^2{}_y + C_1)(\sigma^2{}_x + \sigma^2{}_y + C_2)} \tag{14}$$

$$EPI = \frac{\Gamma(\Delta s.\Delta\bar{s}.\Delta\hat{s}\Delta\bar{\hat{s}})}{\sqrt{\Gamma(\Delta s.\Delta\bar{s}.\Delta s.\Delta\bar{s})\Gamma(\Delta\hat{s}.\Delta\bar{\hat{s}}.\Delta\hat{s}.\Delta\bar{\hat{s}})}}$$

$$\Gamma(s_1, s_2) = \sum_{i,j} s_1(i,j)s_2(i,j) \tag{15}$$

Where $\Delta s(i,j)$ *and* $\Delta\hat{s}(i,j)$ are the high pass filter version of the reference and degraded images.

V. RESULTS

Results have been tabulated and comparative chart has been made .Result description table wise is given below

Table I. is for PSNR values in dB tabulated for all the four thresholding scheme considered along with the three different wavelet functions. Fig 3 represents the column chart representation of Table 1.

Table I: PSNR Values in dB For Different schemes

Thesholding Techniques	**DWT**		
	Haar	Db4	Sym4
Visue Shrink	29.05	30.51	31.9
Bayes Shrink	37.99	38.22	39.12
Neighbour Shrink	37	38.77	40.13
Modified Neighbour Shrink	39.63	40.34	41.98

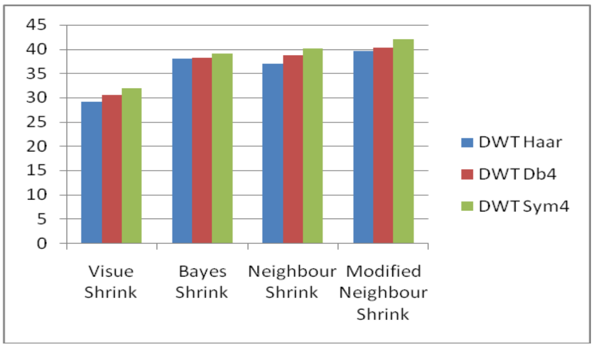

Fig 3: Comparison of PSNR Values in dB for Different schemes

thresholding scheme considered along with the three different wavelet functions. Fig 4 represents the column chart representation of Table II.

Table.II: MSE Values For Different schemes.

Thesholding Techniques	DWT		
	Haar	Db4	Sym4
Visue Shrink	83.6	64.9	50.8
Bayes Shrink	13.4	12,9	11,6
Neighbour Shrink	13.99	11.07	10.9
Modified Neighbour Shrink	9.08	8.69	8.07

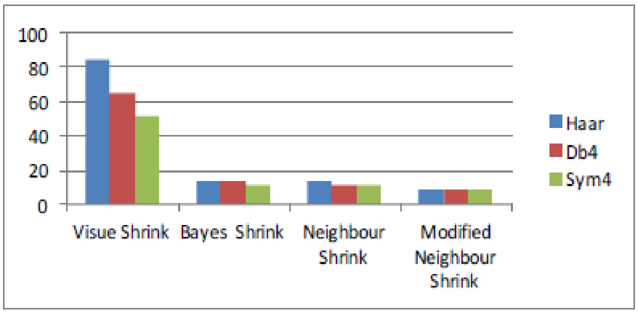

Fig . 4: Comparison of MSE Values for Different schemes

Table III. is for SSIM values tabulated for all the four thresholding scheme considered along with the three different wavelet functions. Fig5.represents the column chart representation of Table III.

Table.111. SSIM Values For Different schemes.

Thesholding Techniques	DWT		
	Haar	Db4	Sym4
Visue Shrink	0.5566	.643	.7041
Bayes Shrink	0.9326	.94	.9489
Neighbour Shrink	0.92528	.9502	.959
Modified Neighbour Shrink	0.9538	.967	.978

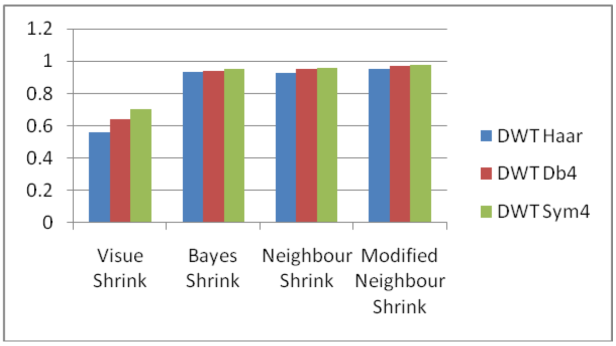

Fig 5. Comparison of SSIM Values for Different schemes

Table IV. is for EPI values tabulated for all the four thresholding scheme considered along with the three different wavelet functions. Fig 6. represents the column chart representation of Table IV.

Table IV: EPI Values For Different schemes.

Thesholding Techniques	DWT		
	Haar	Db4	Sym4
Visue Shrink	0.3034	.498	.567
Bayes Shrink	0.6767	.7034	.7267
Neighbour Shrink	0.7021	.72	.75
Modified Neighbour Shrink	0.7513	0.7632	0.7809

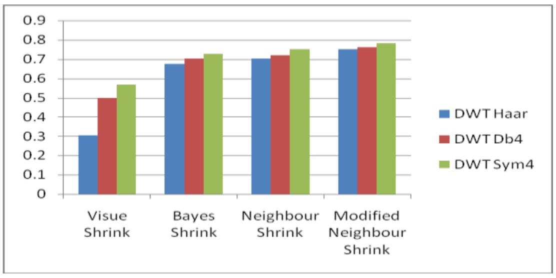

Fig .6: Comparison of EPI Values for Different schemes

Table V. is for MSE and PSNR values tabulated for all the four thresholding scheme considered along with the Haar DWT. Fig 7. represents the column chart representation of Table V.

Table. V: MSE and PSNR Values For Different schemes.

DISCRETE WAVELET TRANSFORM (Haar)		
Thresholding Techniques	MSE	PSNR in dB
Visu Shrink	83.6	29.05
Bayes Shrink	13.4	37.99
Neighborhood Shrink	13.99	37
Modified Neighborhood Shrink	9.08	39.63

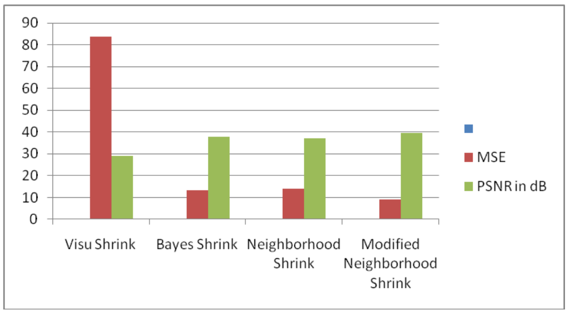

Fig .7: Comparison of MSE and PSNR in dB for Different schemes

Table VI. is for SSIM and EPI values tabulated for all the four thresholding scheme considered along with the Haar DWT. Fig 8. represents the column chart representation of Table VI.

Table. VI. SSIM and EPI Values For Different schemes.

DISCRETE WAVELET TRANSFORM (Haar)		
Thresholding Tech.	SSIM	EPI
Visu Shrink	0.5566	0.3034
Bayes Shrink	0.9326	0.6767
Neighborhood Shrink	0.92528	0.7021
Modified Neighborhood Shrink	0.9538	0.7513

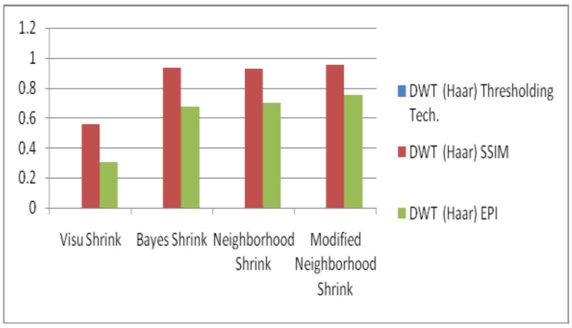

Fig. 8 Comparision of SSIM and EPI for different schemes

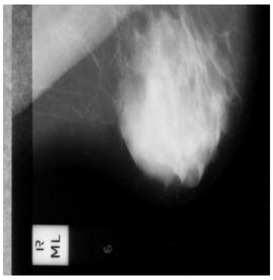

Fig 9 (a) Original Image

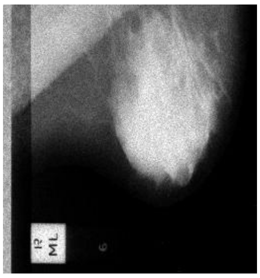

Fig 9 (b) Noised Image

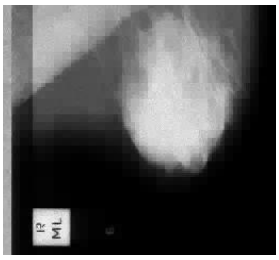

Fig 9 (c) Visu Shrink Denoised Image

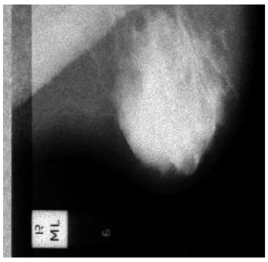

Fig 9 (d) Bayes Shrink Denoised Image

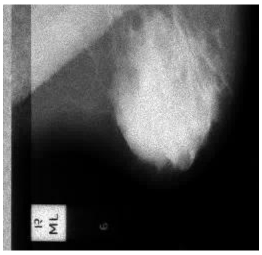

Fig 9 (e) Neighbour Shrink Denoised Image

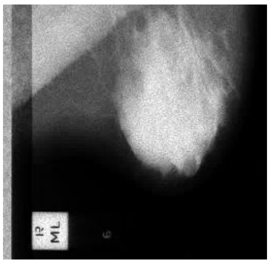

Fig 9(f) Modified Neighbour Shrink Denoised Image

VI. CONCLUSIONS

As per the tabular and chart representation of Results the Following observations are made

- As the shrinkage function has been considered
- Visu shrink gives the poorest performance for every performance indices as compared to other shrinkage functions.
- Modified Neighbourhood Shrinkage Function gives the best results for all the performance indices like PSNR, MSE, SSIM and EPI.
- As different wavelets considered the Haar gives the poorest performance among the other considered functions.
- Sym4 gives the best among the other selected wavelet functions. But here improvement is very nominal as compared to the large improvement resulted while choosing the different shrinkage functions.

All the algorithms have been run on MIAS [12] , data base and some sample images and tables for some images has been represented as the sample observations. MATLAB has been used for simulations.

As said, to insert images in *Word*, position the cursor at

Sr. No	Image No	DISCRETE WAVELET TRANSFORM															
		Visu Shrink				Bayes Shrink				Neighborhood Shrink				Modified Neighborhood Shrink			
		MSE	PSNR in dB	SSIM	EPI	MSE	PSNR in dB	SSIM	EPI	MSE	PSNR in dB	SSIM	EPI	MSE	PSNR in dB	SSIM	EPI
1	mbd 1	67.28	29.85	0.592	0.233	10.78	37.8	0.946	0.6407	8.92	38.62	0.96	0.6863	6.01	40.33	0.975	0.7405
2	mbd 2	69.04	29.72	0.669	0.323	7.037	39.65	0.96	0.7474	6.89	39.47	0.943	0.7639	4.57	39.74	0.959	0.8076
3	mbd 3	57.37	30.54	0.719	0.383	3.53	42.64	0.985	0.8168	3.616	42.54	0.98	0.8264	2.5	44.13	0.986	0.855
4	mbd 4	73.63	29.46	0.64	0.317	5.943	40.39	0.975	0.772	5.97	40.37	0.971	0.7853	3.94	42.17	0.9803	0.8246
5	mbd 5	115.61	27.5	0.363	0.124	30.78	33.24	0.835	0.503	33.75	32.84	0.8078	0.5099	22.1	34.67	0.887	0.601
6	mbd 6	129.7	26.999	0.354	0.124	32.84	32.96	0.837	0.513	38.69	32.25	0.793	0.5807	25.12	34.12	0.875	0.6043
7	mbd 7	61.42	30.247	0.663	0.306	4.84	41.27	0.977	0.777	4.84	41.27	0.975	0.789	3.24	43.01	0.9837	0.8284
8	mbd 8	104.13	27.95	0.48	0.201	16.17	36.04	0.925	0.643	16.08	36.01	0.924	0.6617	10.377	37.96	0.954	0.7281
9	mbd 9	74.21	29.42	0.587	0.28	7.2	39.55	0.965	0.733	8.043	39.07	0.956	0.7348	5.325	40.867	0.972	0.7805
10	mbd 10	83.65	28.9	0.499	0.743	14.93	36.38	0.921	0.622	11.7	37.48	0.943	0.683	7.629	39.3	0.966	0.743

Fig10. Complete Data Set For 10 Sample Images Denoising with Haar.

Poisson's Noise, being the signal dependent, gives different simulation time for different images as well as different threshold value also. So direct comparisons of these parameters are not possible

ACKNOWLEDGMENT

Authors are very thankful to MIAS for providing such a big data base of Mammographic Images free for research purposes.

REFERENCES

1. World Health StaticticsTech. rep. World Health Organization(WHO),(2013). http://www.who.int/gho/publications/world_health_statistics
2. Mortton M., Whaley, K. Brandt, and K. Amrami," Screening mammograms: Interpretation with computer-aided detection—Prospective evaluation", Radiology, vol. 239, no. 2, (2006), pp 375–383.
3. Pisano E.D., Hendrick R. E., Yaffe M, Conant E.F. & Gatsonis C., "Should breast imaging practices convert to digital mammography?, A response from members of the DMIST executive committee", Radiology, vol. 245, no. 1,(2007) , pp. 12–13.
4. Mencattini A., Salmeri M., Lojacono R. , Frigerio M. , & F. Caselli F., "Mammographic images enhancement and denoising for breast cancer detection using dyadic wavelet processing," IEEE Transactions on Instrumentation and Measurement, vol. 57, no .7, (2008) pp 1422 – 1430.
5. Strang G. & Nguyen T.Q., Wavelets and Filter Banks, Wellesley-Cambridge Press, (1998) Wellesley, MA, Revised Edition.
6. Donoho D.,"De-noising by soft thresholding", IEEE Trans. on Information Theory, vol. 38(2), (1995) , pp. 613-627.
7. Donoho D & Johnstone I.,"Ideal spatial adaptation by wavelet shrinkage", Biometrikavol .81(3), ,(1994) pp 425-455.
8. Vetterli M. "Wavelets and Filter Banks: Theory and Design ",IEEE Trans. on Signal Processing, vol. 40, (1992), pp.2207-2232.
9. Soman K.P., Ramchandran K.I. & Reshmi N.G. "Insight into Wavelets from Theory to Practic". PHI Learning Private Limited, (2013) New Delhi. Third Edition.
10. Saha M., Naskar M. K.,& Chatterji B. N. "Soft, Hard and Block Thresholding Techniques for Denoising of Mammogram Images", IETE Journal of Research, (2015) vol. 61, issue 2, pp 186-191
11. Vaidyanathan P.P., Multirate Systems and Filter Banks, Prentice Hall,(1993) Englewood Cliffs, NJ.
12. Mammographic Image Analysis Society, Available at http://www.mammoimage.org/databases/

AUTHORS PROFILE

Smriti Bhatnagar received her M.E. from MNREC Allahabad, India in 1994. Her research interests include Signal Processing and Embedded System Design .
Since July 2003, she has been working as Assistant Professor in the Department of Electronics and Communications Engineering, JIIT, Noida. She has published several research papers in International Journals and presented many in International and National Conferences. She has co- authored a book titled "Control Systems" for undergraduate engineering students.

She is a Fellow member of 'The Institution of Electronics and Telecommunication Engineers (IETE)' India and a member of' IEEE

Richa Gupta has received her Ph.D. Degree from JIIT, Noida, India in the year 2013 and M.Tech in Information Systems from IIT, Kanpur, India in 2005. She obtained her B.Tech degree in ECE from KIET, Ghaziabad, India in 2003, with a special acknowledgement for being the University topper of B.R. Ambedkar University, Agra. She is a distinction holder in her entire academic career. Since August 2007, she has been working as Assistant Professor in the Department of Electronics and Communications Engineering, JIIT Noida. Prior to this, she has worked with a USA based research company 'ATC Labs, Noida' for 2 years